Numerical simulation of filler metal droplets spreading in laser brazing

Yanbin Chen (陈彦宾), Xiaosong Feng (封小松), and Liqun Li (李俐群)

State Key Laboratory of Advanced Welding Production Technology, Harbin Institute of Technology, Harbin 150001

Received May 21, 2007

A finite element model was constructed using a commercial software Fidap to analyze the Cu-base filler metal droplet spreading process in laser brazing, in which the temperature distribution, droplet geometry, and fluid flow velocity were calculated. Marangoni and buoyancy convection and gravity force were considered, and the effects of laser power and spot size on the spreading process were evaluated. Special attention was focused on the free surface of the droplet, which determines the profile of the brazing spot. The simulated results indicate that surface tension is the dominant flow driving force and laser spot size determines the droplet spreading domain.

OCIS codes: 350.3390, 140.3390.

As a novel high temperature brazing technique, laser brazing has the properties of rapid heating and narrow heat-affected zone (HAZ), which are advantages to join coated metal sheets[1,2]. However, because of the difficulties in experimental measurements, a comprehensive understanding of the laser brazing process is difficult and numerical simulation is an effective tool. The simulated results of laser melting, arc brazing, and laser welding were given, and the free surface of the melted material was assumed to be rigid or be solved with the hypothesis of balance state or isothermal state[3−5]. In this paper, a finite element method (FEM) model is developed to investigate the spreading, fluid flow, and temperature distribution of filler metal with stationary laser heating. Detailed information of temperature and fluid flow is calculated to gain a better understanding of the spreading process of filler metal droplets. The free surface deformation and droplet spreading on the base metal surface were considered simultaneously, which is helpful to treat the homogeneous problems in laser soldering.

In laser brazing process, a certain amount of filler metal is put on the galvanized steel sheets which are the base metal, and is heated with a stationary laser beam in a period of time. The filler metal is melted and then spreads under the beam heating, in which heat source is CO_2 laser and $CuSi_3$ is the filler metal. The process is different from laser brazing with filler wire, but it is significant to understand the mechanism of the brazing process with filler wire. The experimental results in early stage indicate that if the filler metal can be melted and spread, increasing the laser heating time has slight influence on droplet spreading diameter[6]. So, in this paper, the spreading process is supposed as steady state, and the droplet initial shape has no effect on the spreading shape, which can be assumed to be a spherical crown (see Fig. 1), and the process can be treated as an axisymmetrical model. Figure 2 shows the model coordinates.

The computed domain is the melted filler metal and the model boundary is composed of the free surface of the droplet, interface between filler metal and base metal, and symmetrical plane. On the free surface, laser heat flux can be treated as boundary condition of the model, and the heat flux distribution is Gaussian. In addition to laser heat flux, irradiation and convection heat transfer are also being considered on the free surface. At the interface, there is heat transfer between filler metal and base metal. However, the base metal is not the computed domain in this model, so irradiation and convection are also imposed on the interface to approximate this heat transfer. The symmetrical plane is loaded as adiabatic boundary conditions.

In melted filler metal, buoyancy, gravity, and surface tension are flow driving force. In the case of small size, thermocapillary convection is the main mechanism of energy and mass transfer in the melted filler metal.

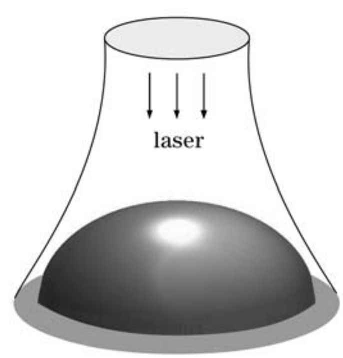

Fig. 1. Schematic of droplet spreading with laser heating.

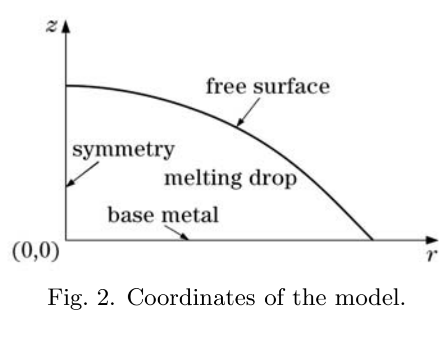

Fig. 2. Coordinates of the model.

Temperature gradient exists on the free surface and different temperatures correspond to the different surface tensions, so surface tension gradient is formed on the free surface, which produces Marangoni convection. On the free surface, Marangoni force balances with viscous shear stress and can be used as momentum boundary condition:

$$\mu\frac{\partial u}{\partial z} = -\frac{\partial \gamma}{\partial T}\cdot\frac{\partial T}{\partial r}, \quad \mu\frac{\partial v}{\partial r} = -\frac{\partial \gamma}{\partial T}\cdot\frac{\partial T}{\partial z}, \qquad (1)$$

where γ is the surface tension, u and v are the fluid flow velocities. At the symmetric plane, radial velocity is set to zero. Flow velocity is zero at the interface because the fluid adheres to the solid base metal. The momentum boundary conditions of the model is imposed.

In the model, gravity and buoyancy are body force and are considered as source item adding to the governing equation of momentum. With Boussinesq approximation, buoyancy can be shown as

$$F_{\mathrm{b}} = (\rho - \rho_{\mathrm{ref}})g = \rho g \beta (T - T_{\mathrm{ref}}), \qquad (2)$$

where ρ_{ref} is the reference density, T_{ref} the reference temperature, β the thermal expansion coefficient, and g the gravity acceleration.

In the commercial software Fidap, spine method is utilized to track or guide the free surface, which is the general method to solve free surface problem with FEM. Spines are lines passing through the free surface nodes which determine a direction for the surface to move. In deformable mesh, all of the nodes on the free surface and under the free surface are located on the spines, and move along the spines. The node distance ratio is a constant when the nodes move along the spines, which is determined by initial mesh. With the spine method, when the free surface deforms, the interior grid is remeshed at the same time. Figure 3 shows the initial mesh, in which the computed domain is divided into the fixed mesh and deformable mesh, and the free surface is the mesh boundary.

The above energy and momentum boundary, source items and free surface treatment method are employed to build a FEM model for simulating the thermal-fluid coupling in laser brazing. The effects of laser power and laser spot size on the droplet spreading process are evaluated. Supposing the process is steady state, all the simulated results are the final steady results. Figure 4 shows the filler metal spreading profile and flow velocity vector in droplet, in which laser power P is 600 W and spot diameter d is 4 mm. After wetting and spreading on the

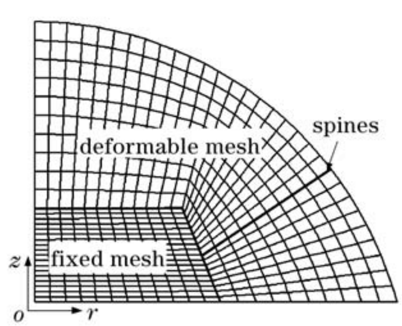

Fig. 3. Generated mesh for laser brazing.

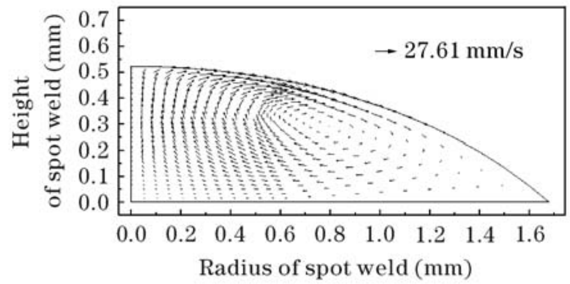

Fig. 4. Fluid flow field in the melted filler metal (P = 600 W, d = 4 mm).

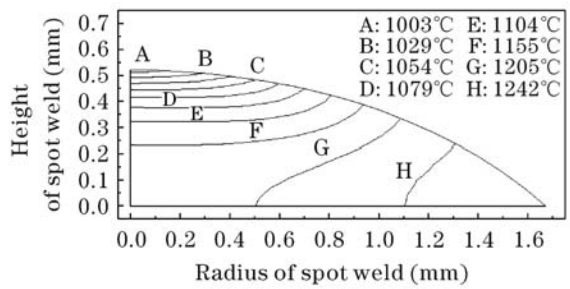

Fig. 5. Temperature distribution of filler metal (P = 600 W, d = 4 mm).

galvanized steel sheet, the melted filler metal forms the shape. Figure 5 shows the temperature distribution of the droplet. The temperature gradient can be found on the free surface, which can lead to surface tension gradient and induce the Marangoni flow. The maximal flow velocity is 27.61 mm/s locating on the free surface.

With heating the large laser spot with diameter of 4 mm, the peak temperature is 1242 °C, appearing on the droplet center top surface as shown in Fig. 5. Maximal temperature gradient is located at the top part of the droplet adjacent the center line. It may be induced by the opposite direction of fluid flow and heat transfer, which impedes the energy transmission from top surface to droplet deep.

Figure 6 shows the flow velocity vector and droplet shape with 800-W laser power and 2-mm spot diameter. The simulated results indicate that decreasing the heating area can lead to the reducing of droplet spreading diameter. The flow situation is roughly similar to that in Fig. 4 and the maximal flow velocity is larger (56.5 mm/s), about twice of laser brazing with 2-mm diameter beam heating, and also located at the free surface of the

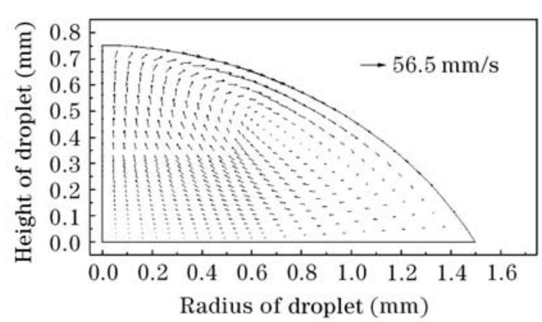

Fig. 6. Fluid flow field in the melted filler metal (P = 800 W, d = 2 mm).

droplet. On the one hand, greater temperature gradient on the free surface is obtained; on the other hand, there is greater circumfluence space between the free surface and the interface. So, larger flow velocity can be obtained with greater laser power and smaller laser spot size.

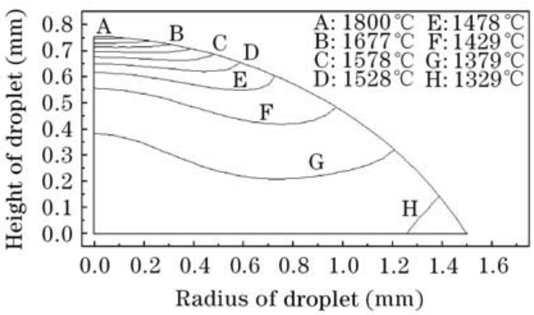

Fig. 7. Temperature distribution of filler metal ($P = 800$ W, $d = 2$ mm).

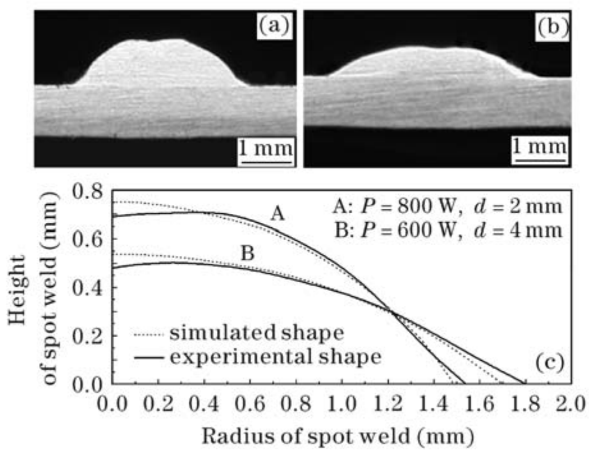

Fig. 8. Comparison between experimental droplet shape and simulated shape. (a) $P = 800$ W, $d = 2$ mm; (b) $P = 600$ W, $d = 4$ mm; (c) comparison between experimental and simulated spot weld shapes.

Figure 7 shows the isothermal cure distribution with 800-W laser power and 2-mm spot diameter. It can be found that the temperature is higher and the influence of fluid flow on the shape of isothermal cures is more significant.

The comparison between experimental droplet shape and simulated droplet shape are shown in Fig. 8. There is a little collapse on the top of the droplets which may be induced by the volume contraction of filler metal in cooling process, which are not considered in the model. Overall speaking, the calculation results is in good agreement with the experimental results.

In conclusion, FEM can be used to simulate the filler metal spreading with free surface shape in non-isothermal laser brazing, and the calculated droplet shape fits well with the experimental result. Increasing laser power and reducing laser spot diameter can lead to larger flow velocity and smaller spreading diameter of the droplet. The maximal flow velocity magnitude is 1 cm/s and laser beam heating area determines the droplet spreading diameter.

This work was supported by the National Natural Science Foundation of China under Grant No. 50275036. X. Feng's e-mail address is fxsupc@hit.eud.cn.

References

1. H. Hanebuth, P. Hoffmann, and M. Geiger, Proc. SPIE **2207,** 146 (1994).
2. X. Feng, L. Li, Y. Chen, and S. Zhou, China Welding **14,** 9 (2005).
3. S. Safdar, L. Li, and M. A. Sheikh, J. Phys. D **40,** 593 (2007).
4. Z. Yu, R. Li, K. Qi, and F. Zhou, Trans. Nonferrous Met. Soc. China **15,** 818 (2005).
5. H. Wang, Y. Shi, and S. Gong, Chin. J. Lasers (in Chinese) **34,** 564 (2007).
6. X. Feng, L. Li, Y. Chen, and S. Zhou, Appl. Lasers (in Chinese) **24,** 357 (2004).